JPP Journal of Pharmacy and Pharmacology

ROYAL PHARMACEUTICAL SOCIETY

JPP Journal of Pharmacy and Pharmacology

JPP 2011, 63: 33–40

Received November 24, 2009
Accepted July 28, 2010
DOI
10.1111/j.2042-7158.2010.01180.x
ISSN 0022-3573

Research Paper

RGD modified albumin nanospheres for tumour vasculature targeting

Praveen K. Dubey[a], Deepak Singodia[b], Rahul K. Verma[b] and Suresh P. Vyas[c]

[a]Novel Drug Delivery Systems Laboratory, Strides Arcolab Limited, Bangalore, Karnataka, [b]Pharmaceutics Division, Central Drug Research Institute (CDRI), Lucknow, and [c]Drug Delivery Research Laboratory, Department of Pharmaceutical Sciences, Dr Harisingh Gour University, Sagar, India

Abstract

Objectives Cyclic arginine-glycine-aspartic acid (RGD) peptide-anchored sterically stabilized albumin nanospheres (RGD-SN) have been investigated for the selective and preferential presentation of carrier contents at angiogenic endothelial cells overexpressing a_vb_3 integrins on and around tumour tissue. Their targetabilty was assessed.

Methods Albumin nanospheres were formulated, conjugated with RGD/RAD peptide and characterized on the basis of size and size distribution. The control Arginine-Alanine-Aspartic acid (RAD) peptide-anchored sterically stabilized nanospheres (RAD-SN) and nanosphere with 5 mol% PEG (SN) without peptide conjugate were used for comparison with RGD-SN for in vitro cell binding, in vivo organ distribution and tumor angiogenesis studies.

Key findings The average size of all nanospheres prepared was approximately 100 nm and maximum drug entrapment was 67.2 ± 5.2%. In-vitro endothelial cell binding of nanospheres exhibited 8-fold higher binding of RGD-SN to human umbilical vein endothelial cells in comparison with the SN and RAD-SN. RGD peptide-anchored nanospheres were significantly ($P \leq 0.01$) effective in the prevention of lung metastasis, angiogenesis and in effective regression of tumours compared with free fluorouracil, SN and RAD-SN. Results indicated that cyclic RGD peptide-anchored sterically stabilized nanospheres bearing fluorouracil were significantly ($P \leq 0.01$) active against primary tumour and metastasis than the nontargeted sterically stabilized nanospheres and free drug.

Conclusions Cyclic RGD peptide-anchored sterically stabilized nanospheres appears promising for targeted cancer chemotherapeutics.

Keywords albumin nanospheres; angiogenesis; cancer chemotherapeutics; cyclic RGD peptide; tumour targeting

Introduction

The most promising application of nanoparticles is to deliver chemotherapeutic agents to the tumour.[1] Nanoparticles exhibit attractive properties such as high stability and the ability to modify their surface characteristics easily. Various natural polymers e.g. bovine serum albumin, chitosan, alginate, etc. have been studied as possible means of targeting drugs to specific sites in the body, with particular emphasis on cancer chemotherapy.[2] Albumin nanospheres have been studied extensively as being suitable for drug delivery.[3–7] They are biodegradable in nature, relatively easy to prepare and their size range can be controlled by varying the preparation conditions.[8,9] They are reported to be relatively nontoxic and produce no short-term adverse immunological response on serial injection.[10] Selective delivery of drugs to target cells can be achieved through antibody guided delivery of nanospheres. Similarly, serum proteins or antibody fragments that recognize specific determinants on target cells can be used for specific delivery. However, attachment of antibodies and larger proteins to the exterior of nanospheres has its own set of problems. Chemistry of protein headgroup–protein coupling is often complex, which jeopardizes the subsequent use of nanospheres in living systems. These chemical interactions may even change confirmation of the protein.

An alternative to the site directing proteins is the use of a defined small peptide domain. Ligand targeting using small peptides has certain advantages over the use of conventional protein macromolecules.[11] These include ease of preparation, lower antigenicity, and increased stability.[12] Argenine-glycine-aspartic acid (RGD) peptides have

Correspondence: Praveen K. Dubey, Novel Drug Delivery Systems Laboratory, Strides Arcolab Limited, Bangalore, Karnataka, 560076, India.
E-mail: pd.praveen@gmail.com

reportedly been used to deliver cytotoxic molecules to the tumour vasculature.[13–15]

Tumour vasculature is a suitable target for targeted cancer therapy because it is composed of nonmalignant endothelial cells that are genetically stable and therefore unlikely to mutate into drug-resistant variants. In addition, these cells are more accessible to drugs and have an intrinsic amplification mechanism. It has been estimated that elimination of a single endothelial cell can inhibit the growth of 100 tumour cells. Tumour vasculature undergoes continuous angiogenesis and express molecular markers that characterize these vessels.[16,17] These markers in angiogenic endothelium include certain receptors for vascular growth factors, such as the receptor for vascular endothelial growth factor and the a_vb_3 integrin.[18,19] Preventing the a_vb_3 integrin from binding to their ligands triggers apoptosis in the endothelial cells of newly formed blood vessels. Peptides that mimic ligands of these integrins and anti-integrin antibodies are capable of inhibiting their ligand binding.

In the last decade, many molecules specifically expressed on to the tumour endothelium cells have been proposed as target molecules for tumour vasculature targeting. The a_vb_3 integrins are overexpressed on actively proliferating endothelium on and around tumour tissue, and have been identified as promising determinants on angiogenic endothelium.[20,21] They can interact with various RGD (Arg-Gly-Asp) sequence containing extracellular matrix components. Synthetic cyclic RGD peptides have been shown to bind selectively to a_vb_3 integrin inhibiting angiogenesis.[22] Various researchers have shown the advantage of using this peptide for significant improvement in targeting for various drugs such as paclitaxel and doxorubicin, but a detailed in-vivo study which could support its translation to the clinic is still lacking.[23,24] Therefore, this study was aimed at designing and developing fluorouracil-bearing sterically stabilized nanospheres anchored with cyclic RGD peptide cyclo(Arg-Gly-Asp-Phe-Lys) (c(RGDfK)) for their selective and preferential presentation at angiogenic tumour endothelial cells, thus assessing their targetabilty.

Materials and Methods

Materials

Bovine serum albumin (BSA), phosphatidylcholine, collagenase and fluorescein isothiocyanate (FITC) were purchased from Sigma Chemicals Company (Sigma, St Louis, USA). *N*-Hydroxysuccinimide-polyethylene glycol-maleimide (NHS-PEG(3400)-MAL) and methoxy-succinimidyl propionate group (mPEG-SPA) were purchased from Shearwater Polymers, Birmingham, AL, USA. Fluorouracil was a gift from M/s Dabur Research Foundation, Ghaziabad, India. Dulbecco's modified Eagle's medium (DMEM), Rosewell Park Memorial Institute (RPMI 1640) medium and fetal calf serum (FCS) were purchased from Hi Media, Mumbai, India. The murine melanoma cell line B16F10 was obtained from the National Center for Cell Science, Pune, India. It was maintained in DMEM supplemented with 10% FCS, 4.5 mg/ml glucose, 2 mM L-glutamine, 100 U/ml benzylpenicillin and 100 mg/ml streptomycin. All other chemicals used were of analytical grade and procured from local suppliers unless mentioned.

Preparation of RGD peptide conjugates

The cyclic RGD peptide cyclo(Arg-Gly-Asp-Phe-Lys) (c(RGDfK)) and control peptide cyclo(Arg-Ala-Asp-Phe-Lys) (c(RADfK)) were synthesized by solid-phase synthesis.[25]

Preparation of fluorouracil-loaded RGD and RAD peptide-coated pegylated nanospheres

Nanospheres of the following compositions were used: cyclic RGD peptide-anchored nanospheres (RGD-SN) composed of BSA/phosphatidylcholine/PEG-RGD (65 : 30 : 5); cyclic RAD peptide-anchored nanosphere (RAD-SN) composed of BSA/phosphatidylcholine/PEG-RAD (65 : 30 : 5); nanospheres with 5 mol% PEG (SN) composed of BSA/phosphatidylcholine/mPEG (2000) (65 : 30 : 5). For in-vitro endothelial cell binding study, 0.1 mol% fluorescently-labelled FITC was added to the BSA.

Preparation of albumin nanospheres

BSA (20% w/v) was dissolved in deionised water. Fluorouracil (0.6% based on albumin weight) was dissolved into BSA aqueous solution. Phosphatidylcholine (10% w/v) solution was prepared in dichloromethane : chloroform (1 : 1). Albumin solution was slowly introduced drop wise in the phosphatidylcholine solution at various hydration ratios ($Wo = [PC]/H_2O$]) under continual stirring so as to obtain a homogeneous micellar dispersion containing albumin dissolved in an apolar aqueous pool of reverse micelles. To rigidize the albumin core, 100 μl 20% solution of a cross-linking agent, glutaraldehyde was added to the micellar dispersion, whilst stirring continued. Various process parameters including hydration ratio, stirring rate, albumin concentration, glutaraldehyde concentration and cross-linking time for their effect on drug loading and size of the final preparation were studied and optimized. The rigidized nanospheres were collected by ultracentrifugation at 60 000 rev/min for 1 h. The nanospheres were washed with diethyl ether. The nanospheres were subsequently redispersed in deionised water and preserved after lyophilization at 4°C. Encapsulation efficiency of prepared nanospheres was determined after digesting nanosphere suspension with trichloroacetic acid and estimating the drug spectrophotometrically at 266 nm.

Anchoring of RGD ligand to nanosphere

Modification of albumin nanospheres with mPEG-SPA and NHS-PEG-MAL

Albumin nanospheres (200 mg) were suspended in 10 ml 0.1 M sodium phosphate at pH 7.5 and allowed to react overnight with 25 μm mPEG-SPA and NHS-PEG-MAL at 4°C.[26] The PEG and PEG-MAL modified albumin nanospheres were collected by ultracentrifugation at 60 000 rev/min for 1 h.

Conjugation of RGD peptides with MPB and PEG-MAL modified nanospheres

Deacetylated cyclic RGD peptide c(RGDfK) and deacetylated cyclic RGD peptide c(RGDfK) in different weight ratios were incubated with MPB-modified PEGylated nanospheres at 4°C

overnight for conjugation of RGD and RAD peptide on to the nanosphere surface.

Vesicle size analysis

The nanospheres were characterized for their size and size distribution by using a Master Sizer 2000 (Malvern Worcestershire, UK).

In-vitro endothelial cell binding of nanospheres

Human umbilical vein endothelial cells (HUVEC) were isolated from human umbilical cord according to a method described previously.[27] In brief, the vein was cannulated and rinsed with buffer solution (140 mmol/l NaCl, 4 mmol/l KCl, 11 mmol/l D-glucose, 10 mmol/l HEPES, pH 7.4). The endothelial cells were detached by 20 min incubation at 37°C with 0.2 mg/ml collagenase resuspended in phosphate-buffered saline (PBS) pH 7.4. The cells were collected, centrifuged (5 min, 200*g*) and cultured at 37°C in 5% CO_2, 95% air humidified atmosphere in RPMI 1640 medium containing 25 mM HEPES, 2 mM L-glutamine supplemented with 20% (v/v) heat-inactivated FCS, 100 IU/ml penicillin, 100 mg/ml streptomycin and 0.25 μg/ml amphotericin B. Nearly confluent monolayers of HUVEC were washed with PBS and cells were detached using 1 mM EDTA in PBS. Cells were subsequently suspended in PBS supplemented with 1% BSA, 1.26 mM $CaCl_2$ and 0.81 mM $MgSO_4$ at 4°C. Cells were counted after centrifugation and 1×10^5 cells were incubated with FITC-labelled SN, RGD-SN and RAD-SN for 1 h at 4°C. The competitive binding experiment with free RGD peptide c(RGDfK) and free RAD peptide c(RADfK) were performed by first incubating the RGD-SN with HUVEC for 30 min, after which 10 000-fold molar excess of either free RGD peptide or RAD peptide was added and the cells were incubated for another 30 min. At the end of the incubation period, cells were washed repeatedly in the supplemented PBS-buffer, fixed with 4% buffered formaldehyde and analysed on a FACScalibur flow cytometer (Becton-Dickinson, NJ, USA).

In-vivo organ distribution studies

Tumour-bearing mice were prepared by injecting B16F10 melanoma cells (2×10^5) cells subcutaneously into the right flank of BALB/c mice (male, 8-weeks-old, 20–25 g). The tumour was allowed to grow until the mean tumour volume was 100 ± 10 mm^3. Animal experiments were carried out using the guidelines of the Council for the Purpose of Control and Supervision of Experiments on Animals (CPCSEA), Ministry of Social Justice and Empowerment, Government of India. The Institutional Animals Ethical Committee of Dr Hari Singh Gour Vishwavidyalaya Sagar, India, approved the protocol and procedures to carry out these studies. The tumour induction model was selected on the basis of United Kingdom/European Union guidelines. All the injectable preparations were sterile and pyrogen free. The free fluorouracil, SN, RGD-SN and RAD-SN were injected intravenously via the tail vein at a dose of 10 mg fluorouracil/kg.

At the selected time post injection, animals were killed and blood was collected by cardiac puncture. The major organs were excised, isolated, washed with Ringer's solution and dried using tissue paper. Organs were stored at –20°C until assay.

Drug estimation in serum

The collected blood samples were centrifuged at 5000 rev/min for 8 min. Serum was harvested from the supernatant. To 150 μl serum, an equal volume of 10% (v/v) trichloroacetic acid in water was added and mixed by vortexing for 30 s. The mixture was then centrifuged at 5000 rev/min for 5 min and the supernatant was filtered through a 0.45-μm membrane filter. A 50-μl sample was injected to a high performance liquid chromatography (HPLC) column. The HPLC equipment consisted of a Beckman Model 116 pump with a 210 A sample injection valve (Beckman, Gagny, France) fitted with a 50 μl sample loop and a Shimadzu SPD-6A spectrophotometric detector. The column was a cation exchange resin in the form of sulfonated styrene-divinylbenzene copolymer (Aminex HPX-87H, 9 μm mean particle diameter, 300×7.8 mm i.d.; Bio-Rad, Ivery-sur-Seine, France) preceded by a similar guard cartridge with UV detection system (265 nm). 5-Bromouracil was used as an internal standard while the mobile phase used was 0.005 M sulfuric acid filtered through a 0.2-μm membrane filter.[28] The flow rate of the mobile phase was 0.5 ml/min.

Estimation of drug in different organs

After removal, various organs (liver, spleen, lungs, kidney and tumour) were weighed and cut into small pieces. One gram of each organ was homogenized with 2 ml PBS (pH 7.4). For organs weighing less than 1 g, the whole organ was used. To 150 μl tissue homogenate an equal volume of 10% (v/v) trichloroacetic acid in water was added and mixed by vortexing for 30 s. The mixture was then centrifuged at 5000 rev/min for 5 min and the supernatant was filtered through a 0.45-μm membrane filter. Tissue homogenate was analysed for drug content as described for serum.

Spontaneous metastasis assay

Spontaneous metastasis was studied by injecting B16F10 melanoma cells (5×10^4) subcutaneously into the right hind footpad of BALB/c mice. Forty mice were divided into four groups of 10. One group of 10 untreated mice was used as the control. Formulations were administered intravenously on day seven after tumour inoculation, and the primary tumours were surgically removed by amputation on day 21. Mice were killed 14 days after the amputation. The lungs were fixed in Bounin's solution and the lung tumour colonies were counted under a Stereozoom microscope (Wild Leitz, Wetzlar, Germany).

Tumour angiogenesis in mice

The assay for tumour angiogenesis in BALB/c mice was carried out following the method described by Kreisle and Ershler[29] with some modification. BALB/c mice were injected intradermally with 5×10^4 B16F10 melanoma cells (through a 27-gauge needle) at two sites on the back. Different formulations were administered intravenously on day two after tumour implantation. Three days after administration of formulations mice were killed immediately after the intravenous injection (0.2 ml) of 0.1% Evans blue and skin was separated from the underlying tissue. Angiogenesis was quantitated by counting the number of vessels oriented towards the

Table 1 Binding of nanospheres with human umbilical vein endothelial cells and effect of free fluorouracil, nanospheres without peptide conjugate, RGD-nanospheres and RAD-nanospheres on angiogenesis by an intradermal injection of B16F10 melanoma

Binding of nanospheres with human umbilical vein endothelial cells		Effect of free fluorouracil, SN, RGD-SN and RAD-SN on angiogenesis by an intradermal injection of B16F10 melanoma	
Formulation	Angiogenesis (no. of vessels)	Formulation	% of maximal human umbilical vein endothelial cells binding
Control	27	SN	17
Free fluorouracil	25	RAD-SN	19
SN	13	RGD-SN	98*
RGD-SN	4*	RGD-SN + free RGD	26
RAD-SN	12	RGD-SN + free RGD	84

Nanospheres without peptide conjugate, SN; RGD-nanospheres, RGD-SN; RAD-nanospheres, RAD-SN. Results are given as means (SD); $n = 5$. *$P \leq 0.01$ compared with other treatments.

tumour mass under a dissecting microscope. All counts were made by a single observer in a blind manner.

Evaluation of antitumor activity

Tumour-bearing mice were divided into groups of 10. Treatment was started when the size of the tumour had reached 100 ± 10 mm^3, approximately on the fourth day after tumour cell inoculation. The dose per injection was 10 mg fluorouracil/kg. Formulations were administered intravenously on day four through the caudal vein. The smallest and largest tumour diameters were measured every second day, using vernier calipers and tumour volume were calculated using the following formula:

$$\text{tumour volume} = 4/3 \times \pi \times (1/2 \times \text{smaller diameter})^2 \times 1/2 \times \text{larger diameter}$$

Survival times were recorded for a total of 80 days after treatment. For histopathological analysis, tumours after treatment were fixed in Bouin's fixative for 8 h and embedded in paraffin. Sections 6 mm wide were cut and stained with haematoxylin and eosin for microscopic analysis.[30]

Statistical analysis

Data have been represented as the mean of 10 individual observations, with standard error of mean. Significance has been calculated using Student's *t*-test.

Results and Discussion

We have developed fluorouracil-loaded and cyclic RGD peptide-anchored sterically stabilized nanospheres for their selective and preferential presentation at tumour vasculature for the effective treatment of cancer. Sterically stabilized nanospheres offered several benefits over conventional nanospheres such as inhibition of the rapid uptake of nanospheres by the reticulo-endothelial system (RES) and reduction of the rate of drug leakage.

In particular, coating the nanospheres with PEG conferred optimal protection to the vesicles from phagocytic cells of the RES. In this study, we have synthesized cyclic RGD peptide c(RGDfK) and control peptide c(RADfK) by solid-phase synthesis. These were purified using reverse-phase HPLC. The purity of the conjugates was estimated to be $98 \pm 0.5\%$. RGD peptide-anchored long circulatory nanospheres (RGD-SN) were prepared using BSA, phosphatidylcholine, NHS-PEG-MAL and c(RGDfK) to improve the circulatory half-life and drug transport capability, while preserving the target affinity of the surface-anchored RGD peptide. Control peptide c(RADfK)-anchored long circulatory nanospheres (RAD-SN) and nanospheres with 5 mol% PEG (SN) without peptide conjugate, but which had similar composition, were used for comparison. It was observed that all nanosphere preparations produced a highly homogeneous population (polydispersity index was 0.163 ± 0.039) with a mean diameter of approximately 101 nm. The maximum drug entrapment was $67.2 \pm 5.2\%$.

Endothelial cell binding was determined by incubating FITC-labelled SN, RGD-SN and RAD-SN with HUVEC. We observed an 8-fold higher binding of RGD-SN to HUVEC in comparison with RAD-SN and SN. Loss of binding affinity in the case of RAD-SN was due to the single amino acid substitution in the RGD peptide. Various researchers exhibited increased affinity and association of RGD modified proteins to proliferating murine endothelial cells expressing a_vb_3 integrins.[24,31] The competitive binding experiment of RGD-SN with free RGD and RAD peptide clearly demonstrated that dissociation of RGD-SN occurred when free RGD peptide was added. This demonstrated that both RGD-SN and free RGD peptide competed for a_vb_3 integrins on human umbilical endothelial cells (Table 1).

Biodistribution of fluorouracil in organs was evaluated in tumour bearing mice until 24 h after injection. Free fluorouracil and different formulations were given to mice through the caudal vein at a dose of 10 mg fluorouracil/kg. As shown in Figure 1, free fluorouracil cleared quickly from the blood. In contrast, in the case of SN and RGD-SN blood levels remained high for a longer period, however, the blood level of RGD-SN was lower than SN. This may have been due to the relatively rapid uptake of RGD peptide-anchored nanospheres by mononuclear phagocytic cells in comparison with SN. As shown in Table 2, RGD-SN level in the spleen was ~2-fold higher ($8.66 \pm 0.76\%$ maximum recovery in 4 h) than SN ($4.18 \pm 0{:}35\%$ maximum recovery in 4 h). This was probably due to the a_vb_3 integrin receptors expression by

mononuclear phagocytic cells in the spleen, responsible for the rapid uptake of RGD-SN.[25] Distribution of SN and RGD-SN in liver, kidney and lungs were not significantly different.

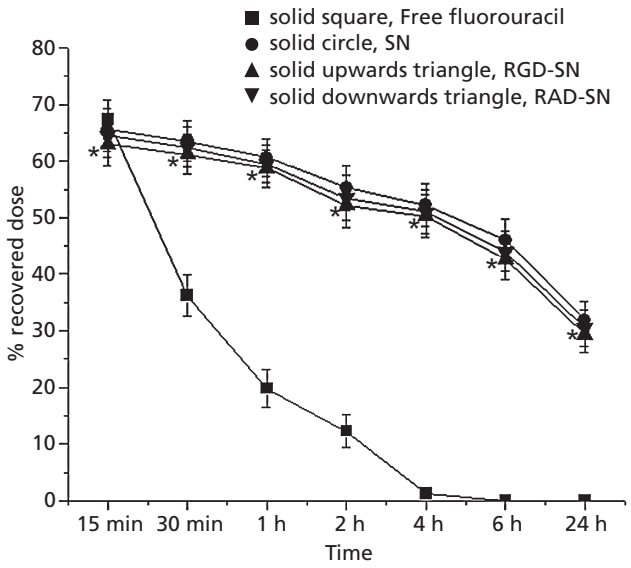

Figure 1 Plasma profiles of fluorouracil (as percent of administered dose) following intravenous injection of different formulations of the drug. The following were injected into tumour-bearing mice at 10 mg fluorouracil/kg: free fluorouracil, nanospheres without peptide conjugate (SN), RGD-nanospheres (RGD-SN) and RAD-nanospheres (RAD-SN). Results are given as means (SD); $n = 3$. $^*P \leq 0.01$, compared with other treatments.

Incorporation of fluorouracil in the nanospheres enhanced the percent administered dose localized in the tumour. Approximately 2.12 ± 0.03% of the administered dose of fluorouracil reached the tumour 30 min after administration of free fluorouracil. This level decreased continuously thereafter. Administration of SN and RAD-SN produced increased accumulation of fluorouracil in tumour (12.4 ± 1.1% and 11.3 ± 0.9% in 6 h) compared with free drug. The highest fluorouracil level (19.12 ± 1.4%) in tumour was obtained 6 h after the administration of RGD-SN. As evident in Figure 2, the RGD concentration was 1.54-fold higher than that of SN and approximately 9.1-times higher than that of free drug. Recently Gao *et al*.[32] showed increased localization of nano-drug in tumour with RGD compared with nano-drug without RGD. Similarly dendrimer-modified gold nanorods conjugated with RGD peptides, showed highly selective targeting and destructive effects on the cancer cells and solid tumours.[33] Increased localization of RGD-SN in the tumour in comparison with SN and free drug may be attributed to the selective and preferential presentation of RGD-SN at tumour vasculature overexpressing a_vb_3 integrin receptors with high affinity for RGD peptide.

We examined the effect of free fluorouracil and different formulations on spontaneous lung metastasis produced by B16F10 melanoma cells, which have a high degree of preference for metastatic growth in the lungs [34] As shown in Table 3, RGD-SN reduced the number of lung colonies to a greater extent (6 ± 3.5 tumour colonies/mouse) in comparison with free fluorouracil and SN (46 ± 13.6 and 25 ± 7.21, respectively). To study metastasis, 10 mice were administered RGD-SN, of these six mice were found to be metastasis free. This experiment showed that RGD

Table 2 Organ distribution after intravenous injection of free fluorouracil, nanospheres without peptide conjugate, RGD-nanospheres and RAD-nanospheres into B16F10 tumour bearing BALB/c mice

Formulation	Organ	Percent dose recovered after						
		15 min	30 min	1 h	2 h	4 h	6 h	24 h
Free fluorouracil	Liver	7.61 ± 0.46	10.1 ± 1.09	8.42 ± 0.75	5.4 ± 0.58	4.2 ± 0.05	ND	ND
	Spleen	0.25 ± 0.06	0.62 ± 0.03	1.12 ± 0.13	0.86 ± 0.07	0.38 ± 0.02	ND	ND
	Lungs	2.1 ± 0.17	2.9 ± 0.02	2.4 ± 0.21	1.9 ± 0.02	ND	ND	ND
	Kidney	ND	2.1 ± 0.01	2.03 ± 0.16	1.55 ± 0.01	1.1 ± 0.01	ND	ND
	Tumour	1.2 ± 0.11	2.12 ± 0.03	1.7 ± 0.13	1.38 ± 0.052	1.14 ± 0.046	ND	ND
SN	Liver	3.8 ± 0.21	5.46 ± 0.34	7.15 ± 0.56	9.3 ± 0.77	11.23 ± 0.89	15.52 ± 1.2	8.69 ± 0.75
	Spleen	0.93 ± 0.04	1.76 ± 0.13	2.12 ± 0.17	3.23 ± 0.23	4.18 ± 0.35	3.33 ± 0.21	1.05 ± 0.06
	Lungs	0.81 ± 0.03	1.36 ± 0.12	1.71 ± 0.14	2.16 ± 0.17	2.3 ± 0.15	1.98 ± 0.11	1.05 ± 0.08
	Kidney	1.46 ± 0.12	2.47 ± 0.17	3.31 ± 0.25	3.14 ± 0.28	3.1 ± 0.21	3.05 ± 0.20	3.04 ± 0.24
	Tumour	2.3 ± 0.21	4.42 ± 0.38	6.63 ± 0.55	9.71 ± 0.78	11.54 ± 1.2	12.4 ± 1.1	7.78 ± 0.65
RGD-SN	Liver	4.32 ± 0.35	6.62 ± 0.54	8.24 ± 0.76	11.17 ± 0.98	12.51 ± 1.3	17.57 ± 1.54	11.71 ± 1.32
	Spleen	2.24 ± 0.16	3.56 ± 0.28	5.46 ± 0.47	6.85 ± 0.53	8.66 ± 0.76	7.31 ± 0.64	2.96 ± 0.18
	Lungs	0.86 ± 0.03	1.48 ± 0.09	2.05 ± 0.23	2.43 ± 0.25	2.58 ± 0.26	2.2 ± 0.18	1.31 ± 0.11
	Kidney	1.23 ± 0.13	2.25 ± 0.23	3.2 ± 0.29	3.02 ± 0.31	2.97 ± 0.27	2.91 ± 0.26	2.87 ± 0.27
	Tumour	3.5 ± 0.32	6.05 ± 0.54	8.4 ± 0.95	12.29 ± 1.22	16.83 ± 1.54	19.12 ± 1.4	10.19 ± 1.16
RAD-SN	Liver	3.9 ± 0.33	5.84 ± 0.55	7.63 ± 0.67	9.85 ± 0.87	11.84 ± 0.96	16.3 ± 1.34	9.53 ± 0.84
	Spleen	1.34 ± 0.14	2.6 ± 0.21	3.21 ± 0.29	4.1 ± 0.38	5.23 ± 0.47	4.71 ± 0.48	2.3 ± 0.17
	Lungs	0.79 ± 0.05	1.7 ± 0.14	2.3 ± 0.24	2.54 ± 0.28	2.63 ± 0.19	2.1 ± 0.22	1.2 ± 0.13
	Kidney	1.51 ± 0.11	2.56v0.22	3.32 ± 0.29	3.55 ± 0.34	3.87 ± 0.40	3.2 ± 0.27	2.6 ± 0.28
	Tumour	2.4 ± 0.23	3.9 ± 0.42	6.3 ± 0.67	9.1 ± 0.66	10.7 ± 0.89	11.3 ± 0.9	6.43 ± 0.34

Dose: 10 mg fluorouracil/kg. Nanospheres without peptide conjugate, SN; ND, not detected; RGD-nanospheres, RGD-SN; RAD-nanospheres, RAD-SN. All the values are representatives of mean ± SD for three independent determinations.

peptide-anchored nanospheres were significantly ($P \leq 0.01$) effective in the control of lung metastasis. These findings were based on the fact that during the metastatic cascade, tumour cells encounter host cells, extracellular matrix and basement membrane components.[35] Synthetic peptides with RGD sequence have been found to have antimetastatic effects, blocking cancer cells binding to extracellular matrix and basement membranes.

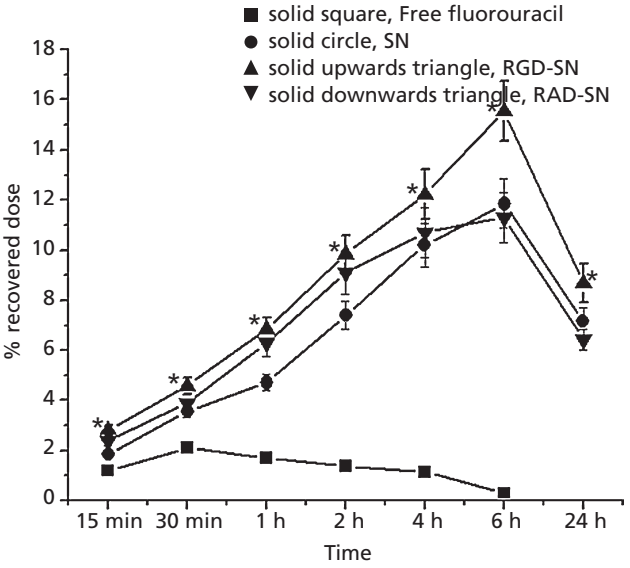

Figure 2 Drug level in the tumour (as % administered dose) following intravenous injection of fluorouracil and different nanosphere formulations of the drug into tumour bearing mice. Nanospheres without peptide conjugate, SN; RGD-nanospheres, RGD-SN; RAD-nanospheres, RAD-SN. Results are given as means (SD); $n = 3$. $P \leq 0.01$. Dose: 10 mg fluorouracil/kg.

Progressive tumour growth and metastasis appears to be associated with the growth of persistent capillary blood vessels (neovascularization) at the primary and metastatic sites, and endothelial cells in the angiogenic vessels within tumours that express several proteins are absent or barely detectable in established blood vessels, including a_vb_3 integrins.[18] Nanospheres equipped with RGD peptide can be targeted to these angiogenic endothelial cells, which have a high affinity for RGD peptide ligand. We therefore examined the effect of different formulations on angiogenesis. Table 1 shows clearly that RGD-SN significantly ($P \leq 0.01$) inhibited angiogenesis as compared with free fluorouracil and SN.

We proceeded further by examining whether RGD peptide targeting to tumour vasculature would result in enhanced antitumour activity of RGD peptide-anchored nanospheres. Fluorouracil, SN, RGD-SN and RAD-SN were administered intravenously on day four at the dose of 10 mg fluorouracil/kg to B16F10 tumour-bearing BALB/c mice. B16 F10 melanoma cell lines were chosen because of their angiogenesis-dependent in-vivo growth.[36,37] Results of the antitumour activity are recorded in Table 4. RGD-SNs were found to have significantly greater tumour-inhibitory effect than free fluorouracil and SN. Treatment with RGD-SN delayed the tumour growth significantly (12 ± 1.32 days) ($P \leq 0.01$) in comparison with fluorouracil and SN (1 ± 0.82 and 5 ± 0.65 days, respectively). Life span was increased significantly ($P \leq 0.01$) in the case of treatment with RGD-SN (108.2%) in

Table 3 Effect of free fluorouracil, nanospheres without peptide conjugate, RGD-nanospheres and RAD-nanospheres on spontaneous lung metastasis in BALB/c mice by an intra-footpad injection of B16F10 melanoma

Formulations	Average no. of metastasis/mouse	Average no. of metastasis/ tumour bearing mouse	No. of metastasis free mice ($n = 10$)
Control	52 ± 15.52	52 ± 15.52	0
Free fluorouracil	46 ± 13.36	46 ± 13.36	0
SN	25 ± 7.21	31.3 ± 6.6	2
RGD-SN	06 ± 3.5*	15 ± 6.32	6
RAD-SN	26 ± 6.78	33.6 ± 8.65	2

Nanospheres without peptide conjugate, SN; RGD-nanospheres, RGD-SN; RAD-nanospheres, RAD-SN. *$P \leq 0.01$ compared with other treatments.

Table 4 Antitumour efficacy of free fluorouracil, nanospheres without peptide conjugate, RGD-nanospheres and RAD-nanospheres in B16F10 melanoma bearing BALB/c mice

Treatment (10 mg/kg)	Time to reach (500 mg)	Tumor growth delay T-C (500 mg)	Survival time (days)		% increase in life span
			Range	Mean	
Control	9 ± 0.9	0	20–40	31.5	0
Free fluorouracil	10 ± 1.2	1 ± 0.14	20–40	33.1	5.08
SN	14 ± 1.3	5 ± 0.65	40–60	48.2	53.01
RGD-SN	21 ± 1.9*	12 ± 1.32	40–60	65.6	108.2
RAD-SN	16 ± 1.7	6 ± 0.78	60–80	52.3	66.03

Dose: 10 mg fluorouracil/kg. Data are the mean (SD) of 10 mice per group. Nanospheres without peptide conjugate, SN; RGD-nanospheres, RGD-SN; RAD-nanospheres, RAD-SN. *$P \leq 0.01$ compared with other treatment.

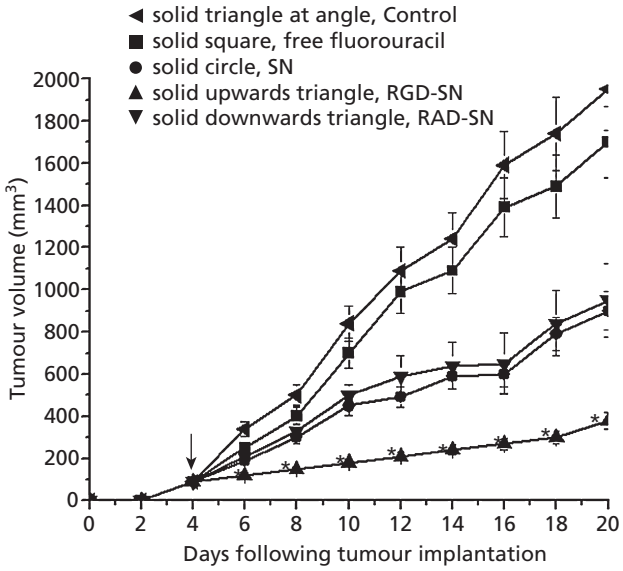

Figure 3 Antitumour efficacy of control, fluorouracil and different nanosphere formulations of the drug in mice bearing B16F10 melanoma. Nanospheres without peptide conjugate, SN; RGD-nanospheres, RGD-SN; RAD-nanospheres, RAD-SN. Arrow represents the time of injection. Results are given as means (SD); $n = 10$. $^*P \leq 0.01$ compared with other treatments.

comparison with free fluorouracil (5.08%) and SN (53.01%). Figure 3 summarizes the relative changes in estimated tumour volume during 28 days of follow-up. Treatment with RGD-SN clearly slowed tumour growth as compared with fluorouracil and SN. These results showed that RGD peptide-anchored nanospheres caused a marked improvement in therapeutic efficacy and growth inhibitory effect on tumour.

Conclusions

The developed system (RGD peptide-anchored sterically stabilized nanospheres) appeared promising in cancer treatment by targeting the tumour vasculature in a mouse model. Studies clearly supported a significant improvement in inhibiting angiogenesis. There was also a decrease in angiogenesis (number of vessels), improvement in HUVEC binding, a decrease in lung metastasis and an increase in the life span of infected mice, clearly justifying this study for further translation for clinical use. Further studies are necessary to establish the possible application of such systems in targeting of anticancer drugs to human tumours.

Declarations

Conflict of interest

The Author(s) declare(s) that they have no conflicts of interest to disclose.

Funding

Praveen K. Dubey is thankful to the Council of Scientific and Industrial Research (CSIR), New Delhi, India, for providing financial assistance (SRF).

Acknowledgements

The Authors are thankful to M/s Dabur Research Foundation, Ghaziabad, India, for the gift sample of fluorouracil. The help and facilities provided by the Head, Department of Pharmaceutical Sciences, Dr H.S. Gour University, Sagar (M.P.), India is duly acknowledged.

References

1. Kreuter J. Nanoparticles and microparticles for drug and vaccine delivery. *J Anat* 1996; 189: 503–505.
2. Tan ML *et al*. Cancer, chitosan nanoparticles and catalytic nucleic acids. *J Pharm Pharmacol* 2009; 61: 3–12.
3. Zonghua L *et al*. Polysaccharides-based nanoparticles as drug delivery systems. *Adv Drug Deliv Rev* 2008; 60: 1650–1662.
4. Lee T *et al*. Serum albumin beads: an injectable biodegradable system for the sustained release of drugs. *Science* 1981; 213: 233–235.
5. Heidrun W *et al*. Tumour cell delivery of antisense oligonucleotides by human serum albumin nanoparticles. *J Control Release* 2004; 96: 483–495.
6. Feng-Qian L *et al*. Mannose 6-phosphate-modified bovine serum albumin nanoparticles for controlled and targeted delivery of sodium ferulate for treatment of hepatic fibrosis. *J Pharm Pharmacol* 2009; 61: 1155–1161.
7. Thakkar H *et al*. Albumin microspheres as carriers for the antiarthritic drug celecoxib. *AAPS PharmSciTech* 2005; 06: E65–E73.
8. Wartlicka H *et al*. Tumour cell delivery of antisense oligonucleotides by human serum albumin next term nanoparticles. *J Control Rel* 2004; 96: 483–495.
9. Tomilson E, Burger JJ. Methods in enzymology. In: Widder K, Green R, eds. *Drug and Enzyme Targeting*. Vol. 112. London: Academic Press, 1995: 27.
10. Shena ZY *et al*. Preparation and characterization of thermo-responsive albumin nanospheres. *Int J Pharmaceutics* 2008; 346: 133–114.
11. Zips D *et al*. Epidermal growth factor receptor inhibitors for radiotherapy: biological rationale and preclinical results. *J Pharm Pharmacol* 2008; 60: 1019–1028.
12. Forssen E, Willis W. Ligand targeted liposomes. *Adv Drug Deliv Rev* 1998; 29: 249–271.
13. Arap W *et al*. Cancer treatment by targeted drug delivery to tumor vasculature in a mouse model. *Science* 1998; 279: 377–380.
14. Ellerby HM *et al*. Anticancer activity of targeted pro-apoptotic peptides. *Natl Med* 1999; 5: 1032–1038.
15. Schiffelers RM *et al*. Anti-tumor efficacy of tumor vasculature-targeted liposomal doxorubicin. *J Control Release* 2003; 91: 115–122.
16. Bertolini F *et al*. Molecular and cellular biomarkers for angiogenesis in clinical oncology. *Drug Discov Today* 2007; 12: 806–812.
17. Shannon AM, Williams KJ. Antiangiogenics and radiotherapy. *J Pharm Pharmacol* 2008; 60: 1029–1036.
18. Brooks PC *et al*. Requirement of vascular integrin avb3 for angiogenesis. *Science* 1994; 264: 569–571.
19. Friedlander M *et al*. Definition of two angiogenic pathways by distinct integrins. *Science* 1995; 270: 1500–1502.
20. Kumar CC *et al*. Targeting integrins alpha v beta3 and alpha v beta 5 for blocking tumor-induced angiogenesis. *Adv Exp Med Biol* 2000; 476: 169–180.
21. Hynes RO. A reevaluation of integrins as regulators of angiogenesis. *Natl Med* 2002; 8: 918–921.

22. Bibby DC *et al*. Surface Pharmacokinetics and biodistribution of RGD-targeted doxorubicin-loaded nanoparticles in tumor-bearing mice. *Int J Pharmaceutics* 2005; 293: 281–290.
23. Danhier F *et al*. Targeting of tumor endothelium by RGD-grafted PLGA-nanoparticles loaded with Paclitaxel. *J Control Release* 2009; 140: 166–173.
24. Cressman S *et al*. Synthesis of a labeled RGD—lipid, its incorporation into liposomal nanoparticles, and their trafficking in cultured endothelial cells. *Bioconjug Chem* 2009; 20: 1404–1411.
25. McCusker FC *et al*. Solid-phase synthesis of cRGDfK. Derivatives: on-resin cyclisation and lysine functionalisation. *Bioorg Med Chem Lett* 2002; 12: 547–549.
26. Miron T, Wilchek M. A simplified method for the preparation of succinimidyl carbonate polyethylene glycol for coupling to proteins. *Bioconjug Chem* 1993; 4: 568–569.
27. Jaffe EA *et al*. Culture of human endothelial cells derived from umbilical veins. Identification by morphologic and immunologic criteria. *J Clin Invest* 1973; 52: 2745–2756.
28. Compagnon P *et al*. Simple high-performance liquid chromatographic method for the quantitation of 5-fluorouracil in human plasma. *J Chromatogr* 1996; 677: 380–383.
29. Kreisle RA, Ershler WB. Investigation of tumor angiogenesis in an id mouse model: role of host tumor interaction. *J Natl Cancer Inst* 1988; 80: 845–849.
30. Gladson CL, Cheresh DA. Glioblstoma expression of vitronectin and the avb3 integrin. *J Clin Invest* 1991; 88: 1924–1932.
31. Kok RJ *et al*. Preparation and functional evaluation of RGD-modified proteins as avb3 integrin directed therapeutics. *Bioconjug Chem* 2002; 13: 128–135.
32. Gao Y *et al*. Synthesis of vascular endothelial cells-targeting nanometer gene drug carrier Tyr-KGD-PEG-PEI and its biological activity. *Yaoxue Xuebao* 2009; 44: 1034–1039.
33. Li Z *et al*. RGD-Conjugated dendrimer-modified gold nanorods for in vivo tumor targeting and photothermal therapy. *Mol Pharm* 2010; 7: 94–104.
34. Fidler I. Selection of successive tumor lines for metastasis. *Natl New Biol* 1973; 242: 148–149.
35. Fidler IJ. The Ernst W. Bertner memorial award lecture: the evolution of biological heterogeneity in metastatic neoplasms. In: Nicolson GI, Milas I, eds. *Cancer Invasion and Metastasis. Biologic and Therapeutic Aspects*. New York: Rason Press, 1984: 5–9.
36. Boehm T *et al*. Antiangiogenic therapy of experimental cancer does not induce acquired drug resistance. *Nature* 1997; 390: 404–407.
37. Streit M *et al*. Thrombospondin-2: a potent endogenous inhibitor of tumor growth and angiogenesis. *Proc Natl Acad Sci USA* 1999; 96: 14888–14893.